Check for updates

Received: 21 February 2024 | Revised: 18 June 2024 | Accepted: 12 July 2024

DOI: 10.1002/psp4.13212

ARTICLE

Modeling of HIV-1 prophylactic efficacy and toxicity with islatravir shows non-superiority for oral dosing, but promise as a subcutaneous implant

Hee-yeong Kim[1] | **Lanxin Zhang**[1] | **Craig W. Hendrix**[2] | **Jessica E. Haberer**[3,4] | **Max von Kleist**[1,5]

[1]Project Group 5 "Systems Medicine of Infectious Disease", Robert Koch Institute, Berlin, Germany

[2]Department of Medicine, Johns Hopkins University School of Medicine, Baltimore, Maryland, USA

[3]Center for Global Health, Massachusetts General Hospital, Boston, Massachusetts, USA

[4]Harvard Medical School, Boston, Massachusetts, USA

[5]Mathematics for Data Science, Department of Mathematics and Computer Science, Freie Universität Berlin, Berlin, Germany

Correspondence
Max von Kleist, Project Group 5 "Systems Medicine of Infectious Disease", Robert Koch Institute, Berlin, Germany.
Email: kleistm@rki.de; max.kleist@fu-berlin.de

Abstract

HIV prevention with pre-exposure prophylaxis (PrEP) constitutes a major pillar in fighting the ongoing epidemic. While daily oral PrEP adherence may be challenging, long-acting (LA-)PrEP in oral or implant formulations could overcome frequent dosing with convenient administration. The novel drug islatravir (ISL) may be suitable for LA-PrEP, but dose-dependent reductions in $CD4^+$ T cell and lymphocyte counts were observed at high doses. We developed a mathematical model to predict ISL pro-drug levels in plasma and active intracellular ISL-triphosphate concentrations after oral vs. subcutaneous implant dosing. Using phase II trial data, we simulated antiviral effects and estimated HIV risk reduction for multiple dosages and dosing frequencies. We then established exposure thresholds where no adverse effects on immune cells were observed. Our findings suggest that implants with 56–62 mg ISL offer effective HIV risk reduction without reducing lymphocyte counts. Oral 0.1 mg daily, 3–5 mg weekly, and 10 mg biweekly ISL provide comparable efficacy, but weekly and biweekly doses may affect lymphocyte counts, while daily dosing regimen offered no advantage over existing oral PrEP. Oral 0.5–1 mg on demand provided > 90% protection, while not being suitable for post-exposure prophylaxis. These findings suggest ISL could be considered for further development as a promising and safe agent for implantable PrEP.

Study Highlights

WHAT IS THE CURRENT KNOWLEDGE ON THE TOPIC?

Islatravir (ISL) is an extremely potent first-in-class nucleoside-reverse-transcriptase-translocation-inhibitor (NRTTI) that may be suitable for infrequent (i.e., weekly) oral dosing as HIV PrEP, or as long-acting (LA-)PrEP when administered as subcutaneous implant. However, lymphopenia was associated with

This is an open access article under the terms of the Creative Commons Attribution-NonCommercial-NoDerivs License, which permits use and distribution in any medium, provided the original work is properly cited, the use is non-commercial and no modifications or adaptations are made.
© 2024 The Author(s). *CPT: Pharmacometrics & Systems Pharmacology* published by Wiley Periodicals LLC on behalf of American Society for Clinical Pharmacology and Therapeutics.

oral 0.75 mg daily, putting PrEP trials on halt and potentially limiting treatment use, although further research is ongoing in this area.

WHAT QUESTION DID THIS STUDY ADDRESS?

We modeled the pharmacokinetics, pharmacodynamics, toxicity, and prophylactic efficacy of ISL to assess the safety and suitability of low oral doses or implant dosing for HIV prevention.

WHAT THIS STUDY ADDS TO OUR KNOWLEDGE?

Our findings suggest that implants with 56–62 mg ISL offer safe, effective HIV risk reduction without risk of lymphopenia. Low doses of oral ISL can be safe but constitute adherence requirements similar to established oral PrEP regimen.

HOW MIGHT THIS CHANGE DRUG DISCOVERY, DEVELOPMENT, AND/OR THERAPEUTICS?

Our work highlights that oral ISL non-toxic doses may not fill a unique prophylactic niche, while implant dosing could be further explored as LA-PrEP. Our modeling may serve as a blueprint for defining the prophylactic niche of second-generation NRTTIs.

INTRODUCTION

Over 40 years after the discovery of HIV as the cause of AIDS,[1,2] the epidemic remains a significant public health concern. By 2022, HIV caused over 85 million infections and 40 million deaths,[3] one every minute.[4] While highly active antiretroviral treatment can prevent AIDS, there is still no cure for HIV nor an effective vaccine.

Pre-exposure prophylaxis (PrEP) has proven effective in preventing HIV transmission when taken as directed.[5] Currently, three options are available: daily or on-demand oral PrEP with emtricitabine/tenofovir disoproxil fumarate (FTC/TDF) or FTC/tenofovir alafenamide (TAF), injectable long-acting cabotegravir (CAB-LA) and a monthly vaginal ring containing dapivirine (DPV-VR).[6] Oral FTC/TDF PrEP is widely available in high-income settings, particularly among men-who-have-sex-with-men (MSM).[7] When taken on demand, it can reduce HIV acquisition risk by ≈ 95%.[8,9] In heterosexual women, the success of FTC/TDF PrEP may be hampered by poor adherence,[10] and on-demand use is currently not recommended by the WHO.[11] However, CAB-LA-PrEP demonstrated an ~94% incidence reduction in heterosexual women,[12] suggesting LA-PrEP as an excellent alternative for those unable to adhere to a daily regimen.

The investigational drug islatravir (ISL, MK-8591 or EFdA) may have considerable potential for LA-PrEP, due to its antiviral potency (sub-nanomolar range), long intracellular half-life and high barrier to drug resistance.[13,14] So far, the pharmacokinetics and antiviral potency of ISL have been assessed for daily, weekly, and monthly oral dosing, and as a subcutaneous implant, which may need to be replaced every 3–6 months. ISL has been viewed by many as a potential "game changer" for HIV prevention, by decreasing barriers to adherence (such as poor access, discrimination, and stigma) and increasing convenience.

ISL is a deoxyadenosine analog that inhibits HIV-1 reverse transcriptase (RT). Unlike approved nucleoside-RT-inhibitors (NRTIs) which act as immediate polymerase chain terminators,[15,16] ISL is a first-in-class nucleoside-RT-translocation-inhibitor (NRTTI).[17,18] After uptake by HIV target cells and tri-phosphorylation into its active form, islatravir-triphosphate (ISL-TP)[19,20] competes with natural dATPs during reverse transcription. With a 2-fluoro group, ISL has increased intracellular stability, lasting ~78.5–128 h. It exerts multiple mechanisms of action (MOA): The 4′-ethynyl group acts as a weak chain terminator, blocking further nucleotide incorporation into the nascent pro-viral DNA. If RT translocation still occurs, the 3′-OH group causes conformational distortions of the RT-primer/template complex leading to delayed chain termination after incorporation of 1–3 additional nucleotides.[21–23]

In 2021, the US Food and Drug Administration (FDA) halted clinical trials[24] after drops in $CD4^+$ T cells and total lymphocyte counts (lymphopenia) were observed in participants receiving ISL alone,[25] or in combination with other antivirals.[26,27] However, new trials were announced that assess lower doses ISL for HIV treatment,[26] including weekly oral administration with doravirine,[27] while PrEP trials were discontinued.

We developed an integrated mathematical model of ISL's pharmacokinetics (PK), pharmacodynamics (PD), prophylactic efficacy, and toxicity using phase I–II clinical data. This model can help guide further consideration of ISL for HIV treatment and/or prevention. We simulated

21638306, 2024, 10, Downloaded from https://ascpt.onlinelibrary.wiley.com/doi/10.1002/psp4.13212 by Robert Koch-Institut, Wiley Online Library on [28/04/2026]. See the Terms and Conditions (https://onlinelibrary.wiley.com/terms-and-conditions) on Wiley Online Library for rules of use; OA articles are governed by the applicable Creative Commons License

multiple dosing schemes for both oral and implant administration, determined dose-dependent adverse effects, and assessed toxicological risks and prophylactic efficacy of low-dose ISL regimens. Our approach may identify a safe and effective niche for ISL, serving as a blueprint to guide the further development of NRTTIs for HIV prophylaxis and treatment.

METHODS

Pharmacokinetic (PK) data

We considered all relevant, publicly available pre-clinical[28] and clinical data on ISL including oral and implant formulations. For single oral doses of 0.5–400 mg, this included 10 datasets on average plasma ISL PK and 11 datasets on intracellular ISL-TP in peripheral blood mononuclear cells (PBMCs), which was used as a marker for the antiviral effect site in HIV PrEP. For subcutaneous implant administration, we examined five loading doses with ISL levels ranging from 48 to 62 mg, including two doses (54 and 62 mg) reporting both plasma ISL and intracellular ISL-TP before and after the implant was removed at week 12. A summary of the utilized PK data is provided in Table S1.

PK modeling

We considered a semi-mechanistic compartmental model to predict plasma ISL and intracellular ISL-TP pharmacokinetics as depicted in Figure 1a with ordinary differential equations outlined below.

$$\frac{\mathrm{d}}{\mathrm{d}t}\mathrm{Impl} = -e^{-k_R \cdot t} \cdot k_{\mathrm{Impl}\to\mathrm{SC}}(\mathrm{ld}) \cdot \mathrm{Impl}\ (\text{implant dosing}) \tag{1}$$

$$\frac{\mathrm{d}}{\mathrm{d}t}\mathrm{SC} = -\frac{\mathrm{d}}{\mathrm{d}t}\mathrm{Impl} - k_{\mathrm{SC}\to C} \cdot \mathrm{SC} - k_{\mathrm{SC}\to\emptyset} \cdot \mathrm{SC}\ (\text{subcutaneous}) \tag{2}$$

$$\frac{\mathrm{d}}{\mathrm{d}t}D = -k_a \cdot D\ (\text{oral dosing}) \tag{3}$$

$$\frac{\mathrm{d}}{\mathrm{d}t}C = k_{\mathrm{SC}\to C} \cdot \mathrm{SC} + \frac{k_a \cdot D}{V_C} + k_{P_1\to C} \cdot P_1 + k_{P_2\to C} \cdot P_2\ (\text{plasma}) - \left(k_{C\to P_1} + k_{C\to P_2} + k_{C\to\emptyset}\right) \cdot C \tag{4}$$

$$\frac{\mathrm{d}}{\mathrm{d}t}P_1 = k_{C\to P_1} \cdot C - k_{P_1\to C} \cdot P_1\ (\text{peripheral I}) \tag{5}$$

$$\frac{\mathrm{d}}{\mathrm{d}t}P_2 = k_{C\to P_2} \cdot C - k_{P_2\to C} \cdot P_2\ (\text{peripheral II}) \tag{6}$$

$$\frac{\mathrm{d}}{\mathrm{d}t}E = k_{C\to E}(\mathrm{dose}) \cdot C - k_{E\to\emptyset} \cdot E\ (\text{effect site}) \tag{7}$$

Implant administration

Subcutaneous ISL implants are placed on the inner side of the non-dominant upper arm. In our PK model, they release ISL (Impl) into the central (plasma) compartment C' via the subcutaneous compartment (SC), Figure 1a. The cumulative drug release from the implant, estimated from an in vitro experiment[28] for non-erodible EVA (ethylene vinyl acetate) at 54 mg and 62 mg loading doses, follows a simple exponential function $k_{\mathrm{Impl}\to\mathrm{SC}}(\mathrm{ld}) \cdot e^{-k_R \cdot t}$, where 'ld' denotes the loading dose. Rates for 48 mg, 52 mg, and 56 mg were linearly interpolated in line with [28] (Table S2). Concentration transfer $\mathrm{SC} \to C$ was modeled by first-order kinetics with rate $k_{\mathrm{SC}\to C}$. Additionally, a perceptible clearance in the subcutaneous compartment at rate $k_{\mathrm{SC}\to\emptyset}$ was included based on the data.

Oral drug dosing

We modeled first-order absorption kinetics with rate parameter k_a from the oral dosing compartment D into the central plasma compartment C, in line with previous studies.[18]

Plasma pharmacokinetics

We considered three compartments (central plasma C, and two phenomenological peripheral compartments P_1, P_2) to model ISL plasma PK after oral or implant dosing. The ISL plasma PK shows a tri-phasic profile, with two phases evident for oral data (Figure 1c) and the third phase only visible for implant administration (Figure 1b). We set the volume of the central compartment to the physiological volume of blood plasma ($V_C = 3.5$ L).[29] The rate parameters for drug transfer between C and P_1 are denoted by $k_{C\to P_1}$ and $k_{P_1\to C}$, respectively. Analogously, $k_{C\to P_2}$ describes the rate constant of ISL transfer of C to P_2, and $k_{P_2\to C}$ the transfer back. The elimination rate constant in the central compartment is denoted by $k_{C\to\emptyset}$.

Intracellular pharmacokinetics

The effect compartment E reflects the concentration of ISL-TP in PBMCs. Influx of plasma ISL into target cells and intracellular conversion to ISL-TP is modeled as dose-dependent input rate parameter $k_{C\to E}(\mathrm{dose})$, while elimination of intracellular ISL-TP is modeled by

21638306, 2024, 10, Downloaded from https://ascpt.onlinelibrary.wiley.com/doi/10.1002/psp4.13212 by Robert Koch-Institut, Wiley Online Library on [28/04/2026]. See the Terms and Conditions (https://onlinelibrary.wiley.com/terms-and-conditions) on Wiley Online Library for rules of use; OA articles are governed by the applicable Creative Commons License

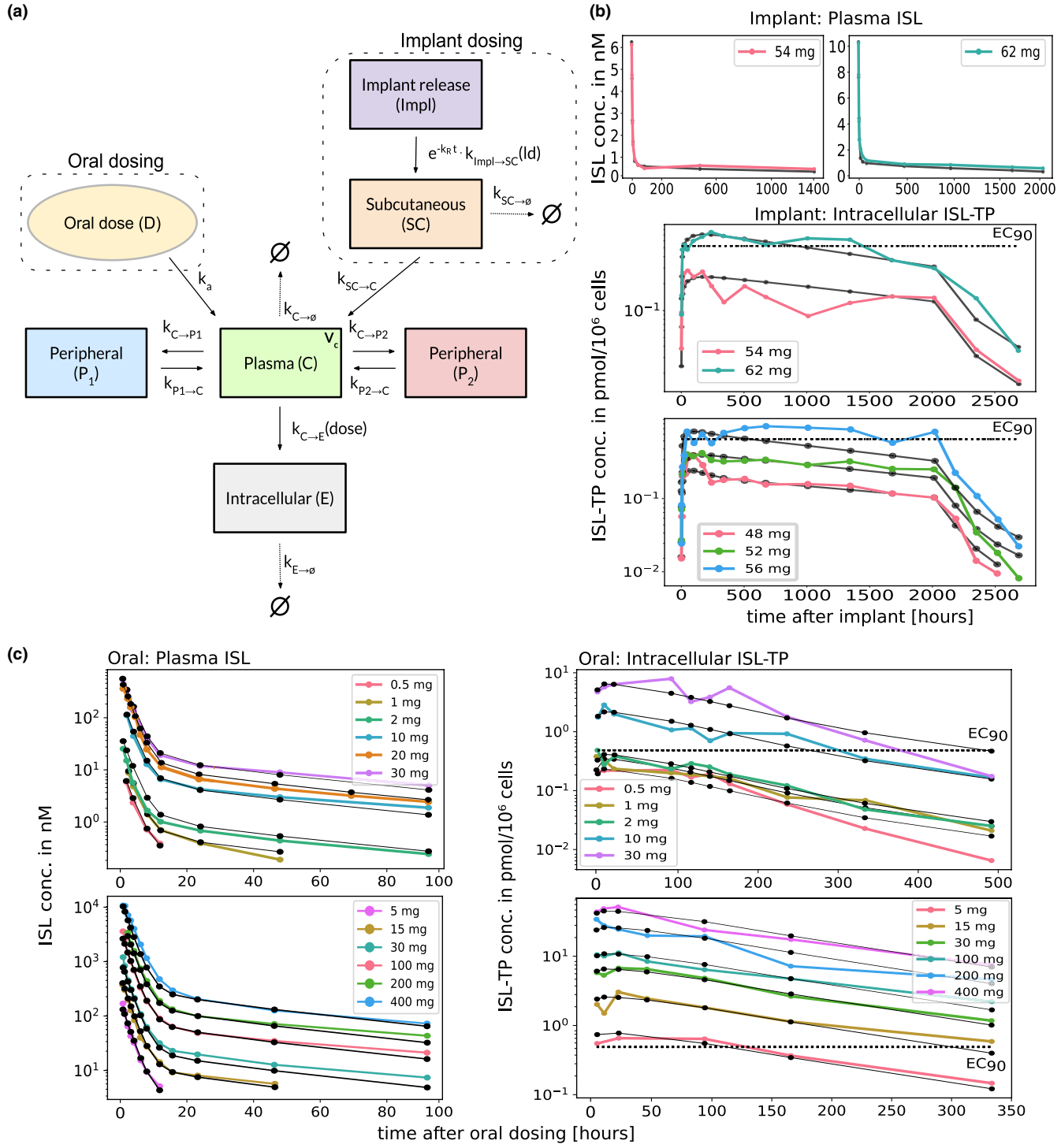

FIGURE 1 Pharmacokinetics of ISL. (a) Integrated pharmacokinetic model encompassing the two routes of drug administration (oral and implant). (b) Clinical (colored-dotted lines) and corresponding model-predicted (black-dotted lines) plasma ISL and intracellular ISL-TP concentrations in PBMCs for implants with different loading doses. Implants were removed after 12 weeks. Data were derived from.[20,31] (c) Clinical (colored-dotted lines) and corresponding model-predicted (black-dotted lines) plasma ISL and intracellular ISL-TP concentrations after single oral doses. The upper panels include data from [19,55] and lower panel from [18]. For reference, model-computed 90% HIV-protective intracellular ISL-TP concentrations (EC_{90}) are shown as dashed horizontal lines on the right-side panels. Average percentage deviation between the data and model predictions were 11.7% for plasma PK and 2.56% for intracellular PK after oral administration and 12.87% and 3.8% for plasma and intracellular data for the implant data.

21638306, 2024, 10, Downloaded from https://ascpt.onlinelibrary.wiley.com/doi/10.1002/psp4.13212 by Robert Koch-Institut, Wiley Online Library on [28/04/2026]. See the Terms and Conditions (https://onlinelibrary.wiley.com/terms-and-conditions) on Wiley Online Library for rules of use; OA articles are governed by the applicable Creative Commons License

first-order kinetics with parameter $k_{E\to\emptyset}$. We ignored any flux of ISL from the cellular into the central compartment, which would only marginally affect plasma PK, due to the very small volume of the PBMC compartment ($\approx 10^{-6}$ L).[30]

Initial conditions

Oral dosing was simulated with the respective initial doses in the dosing compartment D, while all other compartments were either zero (single dose) or set to the pre-dosing concentrations (multiple dose). For implant administration, an initial fraction π_{ld} of the loaded drug $\mathrm{ld} \in \{48,52,54,56,62\}$ in mg was assigned to the subcutaneous tissue, while the rest $\left(1-\pi_{\mathrm{ld}}\right)$ remained in the implant. This drug fraction corresponds to small damage to both implant and tissue, upon insertion. Implant data were available for first- (54, 62 mg) and second-generation (48, 52, 56 mg) formulations. Parameters π_{54} and π_{62} were estimated from first-generation data, comprising plasma and drug release information. The study indicated that the 56 mg implant aimed for similar release rates as the prototype for 62 mg.[31] Consequently, we grouped the remaining π_{ld} values into drug loads ≤ 54 mg and > 54 mg (Table S2).

Viral dynamics and PK-PD link

To infer the antiviral effects of ISL, we used an established HIV-1 viral dynamics model.[29] In essence, this model comprises free infectious virus V, as well as early and late infected T cells and macrophages T_1, T_2, M_1 and M_2. In the viral kinetics model, the process of reverse transcription (hence the transition $V \to T_1$) is inhibited via an Emax model.[32]

$$\eta(t) = \frac{E(t)}{\mathrm{IC}_{50} + E(t)} \tag{8}$$

where $\eta(t)$ denotes the time-dependent strength of inhibition and $E(t)$ denotes the drug concentration at the effect site, compare Equation (7).

Prophylactic efficacy

After estimating viral load (VL) kinetics data based on the HIV-1 viral dynamics system, a reduced model that is sufficient to accurately predict prophylactic efficacy φ[33] was used (more details see Text S1). φ describes the reduction in infection risk per sexual contact, which can be estimated after coupling ISL PK to the viral dynamics model.[29]

$$\varphi\left(Y_0, \mathbf{S}\right) = 1 - \frac{P_I\left(Y_0 \middle| \mathbf{S}\right)}{P_I\left(Y_0 \middle| \emptyset\right)} \tag{9}$$

Infection probabilities can be computed for a particular drug regimen $\mathbf{S}$ or without any drug, denoted as $P_I\left(Y_0 \middle| \mathbf{S}\right)$ and $P_I\left(Y_0 \middle| \emptyset\right)$, respectively. The initial viral state $Y_0 = \left[V, T_1, T_2\right]$ consists of the number of viruses V, early infected T cells T_1 and productively infected T cells T_2.[29] We used a recently developed numerical method[33] to estimate $P_I\left(Y_0 \middle| \mathbf{S}\right)$. Experiments are based on the assumption of a single founder virus.[34]

PK parameter estimation

In a two-step procedure, we estimated all PK parameters (Equation (1)–(7)) based on concentration-time profiles shown in Figure 1b,c using the *trust region reflective method* to minimize the *squared error* between data and model prediction. An outline of the parameter fitting procedure is given in Figure S1.

Parameter boundaries were determined through random parameter seeding and multiple local optimizations to obtain parameter ranges for further optimization. Parameter fitting used plasma drug concentration for implants without transformation, while the remaining data were fitted after log-transformation (Figure 1b,c). Resulting parameter estimates are depicted in Table 1. To facilitate parameter uncertainty quantification by parametric bootstrap, we extracted error estimates in the data, Table S1. We assumed that the data were normal distributed $x \sim \mathcal{N}\left(\mu, \frac{\sigma}{\sqrt{n}}\right)$, where $\frac{\sigma}{\sqrt{n}}$ denotes the sampling error of the data and n denotes the number of samples contributing to the concentration measurement. To address missing values, interpolation was conducted using the coefficient of variation ($\mathrm{CV} = \frac{\sigma}{\mu}$) within or between datasets. If only min/max values were reported, we drew from a uniform distribution.

To estimate bootstrap confidence intervals, we generated 1000 bootstrap samples for each data point and re-fitted the model to each re-sampled dataset. Implant-specific parameters $k_R, \pi(\mathrm{ld}), k_{\mathrm{Impl}\to\mathrm{SC}}(\mathrm{ld})$ were not included in the procedure.

We validated our model using oral ISL data of 0.25–5 mg once daily and 60, 120 mg once monthly, focusing on single-dose experiments and implants, see Figure S2.[35,36]

21638306, 2024, 10, Downloaded from https://ascpt.onlinelibrary.wiley.com/doi/10.1002/psp4.13212 by Robert Koch-Institut, Wiley Online Library on [28/04/2026]. See the Terms and Conditions (https://onlinelibrary.wiley.com/terms-and-conditions) on Wiley Online Library for rules of use; OA articles are governed by the applicable Creative Commons License

Parameter	Value	Parameter	Value
k_a	$0.4232 \pm 8.2 \times 10^{-3}$ (oral)	$k_{C\to P1}$	$1.8494 \pm 9.0 \times 10^{-2}$
$k_{SC\to C}$	$0.0151 \pm 9.0 \times 10^{-4}$ (implant)	$k_{P1\to C}$	$0.0023 \pm 1.0 \times 10^{-2}$
$k_{SC\to \emptyset}$	$0.1521 \pm 1.1 \times 10^{-2}$ (implant)	$k_{C\to P2}$	$5.2726 \pm 1.7 \times 10^{-1}$
$k_{C\to \emptyset}$	$6.8999 \pm 1.9 \times 10^{-1}$	$k_{P2\to C}$	$0.0237 \pm 1.4 \times 10^{-3}$
$k_{E\to \emptyset}$	$0.0088 \pm 3.0 \times 10^{-4}$	V_C	3.5 L (fixed)

TABLE 1 Pharmacokinetic parameter estimates (mean ± standard deviation).

Note: Rate constants are given in the units h^{-1}, the plasma volume V_C was fixed to 3.5 L. The first three parameters depend on the route of administration as noted, the remaining parameters are independent of the dosing route. A detailed description of the rate constants can be found in *Methods*.

PD parameter estimation

To assess ISL's potency, we digitized VL data from phase II 10-day monotherapy trial in HIV-infected subjects ($N = 30$).[19] Using an HIV-1 viral dynamics model, we initially computed steady-state levels in the absence of ISL (pretreatment condition, baseline). By coupling ISL PK with the virus dynamics model (PD) using Equation (8), we estimated the log change in VL from (pretreatment) baseline by fitting the drug potency IC_{50} to the data.[19]

Toxicity thresholds

ISL has been associated with mild, dose-dependent lymphopenia.[37] We specify toxic effects as changes in lymphocyte (and $CD4^+$) cell counts and correlate these effects with plasma ISL levels (details in *Discussion*). Daily oral dosing of 0.25 mg ISL showed no changes in lymphocyte counts.[37] Consequently, we simulated 0.25 mg daily oral dosing and estimated the maximum plasma concentration, serving as no-observed-adverse-effect-level (NOAEL). With this threshold, we calculated the percentage of time above NOAEL for various dosing regimens.

Code and data availability

Codes were written in Python, version 3.10.12, utilizing the SciPy.optimize 1.11.1 and scikit-learn 1.3.0 package. Codes and data are available at https://github.com/KleistLab/ISL_PK-PD-PrEP.

RESULTS

PK model building and parameter estimation

Figure 1a illustrates the derived PK model for both oral and implant dosing with the best-fit parameters in Table 1. All dose-dependent parameters are given in Table S2. Corresponding model-simulated and super-imposed clinical pharmacokinetics are depicted in Figure 1b,c.

Following rapid absorption, the plasma PK exhibits three phases (Figures 1 and S3): The initial phase involves drug distribution from plasma C to peripheral compartments. In this pre-steady state, the transfer rate to the second peripheral compartment $C \to P_2$ surpasses that of the first peripheral compartment $C \to P_1$. The second phase is dominated by $C \to P_1$. Subsequently, concentration exchange between compartments becomes constant, reaching a steady state. The slow elimination of plasma ISL in the steady state is dominated by the flux $P_1 \to C$, with further details in Figure S3.

Intracellular pharmacokinetics are characterized by a rapid uptake and conversion of ISL to ISL-TP and a slow elimination of ISL-TP from the intracellular compartment.

For visual guidance, we depict the concentration that would prevent 90% of infections (EC_{90}), as computed from Figure S4.[38] As shown in Figure 1b,c, single oral doses of ISL smaller than 2 mg and implants with less than 56 mg ISL are not sufficient to produce intracellular concentrations that surpass EC_{90}.

Pharmacodynamics

As a next step, we used the PK model to estimate HIV-1 viral dynamics after single oral doses of ISL as monotherapy. We coupled the model to an established viral dynamics model as outlined in section *Methods* and estimated the potency IC_{50} of ISL-TP in the intracellular compartment (see Figure S5). Parameter estimation yielded $IC_{50} = 429.707 \pm 6.7 \cdot 10^{-5}$ nM. Figure 2 shows predicted VL profiles, incorporating clinical VL dynamics, super-imposed for single oral doses of 0.5, 1, 2, 10, and 30 mg as 10-day monotherapy in HIV-infected individuals.

All considered dosages result in a more than 10-fold VL decline by day 7 post-dose, as reported elsewhere,[19] whereby dose-dependent declines can be observed both

21638306, 2024, 10, Downloaded from https://ascpt.onlinelibrary.wiley.com/doi/10.1002/psp4.13212 by Robert Koch-Institut, Wiley Online Library on [28/04/2026]. See the Terms and Conditions (https://onlinelibrary.wiley.com/terms-and-conditions) on Wiley Online Library for rules of use; OA articles are governed by the applicable Creative Commons License

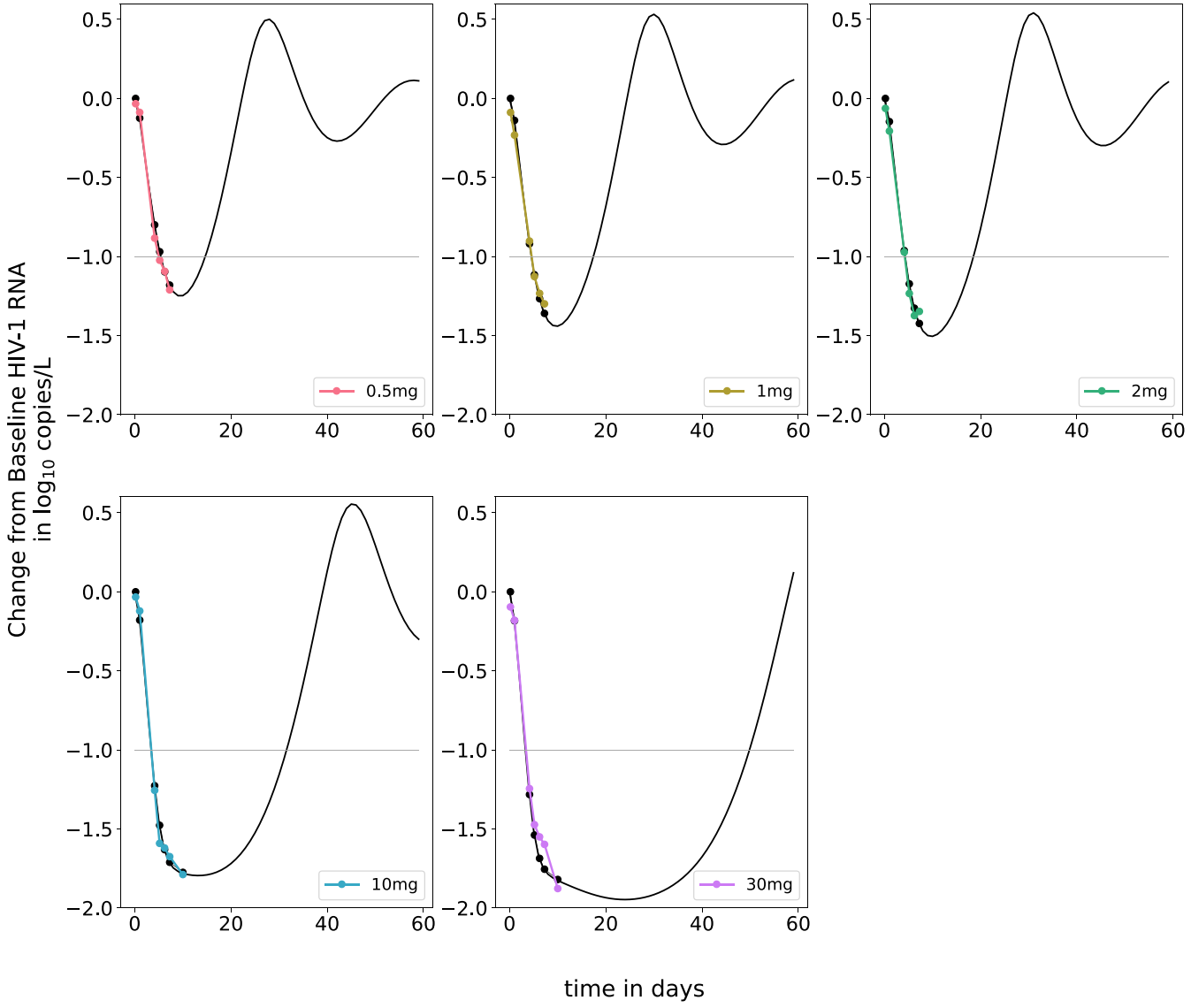

FIGURE 2 Pharmacodynamics of ISL. Mean clinical viral load reductions after a single oral dose of ISL (colored-dotted lines) vs. model-predicted viral load reductions (black-dotted lines). The study included a total of 30 participants (6 per panel/dose), all male and treatment-naive with HIV infection.[19] The horizontal light gray line indicates a 10-fold virus load decline. Viral load data were used to estimate the potency of intracellular ISL-TP IC_{50}, as described in the *Methods*. Average percentage deviation between the data and model predictions was 7.9%.

in the data and simulations. In the simulations, a single oral dose of 30 mg would result in a 100-fold decline in VL 23 days post-dosing.

Predicted PrEP efficacy and toxicity for daily, weekly, biweekly and monthly oral dosing schemes

Recent work[39] using ISL phase II and III data highlighted that daily oral dosing of 0.25 mg ISL resulted in no observable adverse effects on lymphocytes and $CD4^+$ T cell counts. Assuming that plasma ISL is a correlate of toxicity, we found that a maximum plasma concentration of 7.02 nM is reached for daily oral dosing of 0.25 mg ISL. This value was used as a toxicity (NOAEL) threshold.

On the other hand, oral 0.75 mg once daily led to observable decreases in lymphocytes, which were, however, reversible.[37] To evaluate putative toxicity of other daily, weekly and monthly dosing regimens, we computed the percentage of time (at steady state) where the plasma ISL concentration was above the NOAEL of 7.02 nM, as presented in Table 2. We only evaluated dosing regimens that generated plasma ISL levels either below the NOAEL or above the NOAEL for very few time points. Figure 3 (top left) depicts simulated intracellular ISL-TP levels after 0.1, 0.25, and 0.5 mg once-daily dosing. As can be seen from the figure, a daily oral administration of ISL with 0.1 mg would provide a prophylactic efficacy of more than 90% 12 days after the first dose,

21638306, 2024, 10, Downloaded from https://ascpt.onlinelibrary.wiley.com/doi/10.1002/psp4.13212 by Robert Koch-Institut, Wiley Online Library on [28/04/2026]. See the Terms and Conditions (https://onlinelibrary.wiley.com/terms-and-conditions) on Wiley Online Library for rules of use; OA articles are governed by the applicable Creative Commons License

TABLE 2 Summary of derived efficacy vs. toxicity levels for all investigated regimens.

Dose in mg	Drug regimen	Dosing interval τ (in hrs)	Plasma AUC for τ = 24 h	Time above threshold	φ ≥ 90 %	φ ≥ 85 %
0.1	once daily	24	12.99	0.0%	Yes	Yes
0.25	once daily	24	32.49	0.0%	Yes	Yes
0.5	once daily	24	64.97	9.5%	Yes	Yes
0.75	once daily	24	97.46	14.9%	Yes	Yes
2	once weekly	168	36.89	3.4%	No	Yes
3	once weekly	168	55.33	4.2%	Yes	Yes
5	once weekly	168	92.21	5.4%	Yes	Yes
10	once weekly	168	184.44	9.7%	Yes	Yes
15	once weekly	168	276.66	27.1%	Yes	Yes
5	once biweekly	336	46.37	2.6%	No	No
10	once biweekly	336	92.73	4.0%	Yes	Yes
15	once biweekly	336	139.1	8.9%	Yes	Yes
30	once biweekly	336	278.2	25.2%	Yes	Yes
10	once monthly	672	46.22	1.9%	No	No
15	once monthly	672	69.32	3.6%	No	No
30	once monthly	672	138.65	10.8%	No	Yes
60	once monthly	672	277.29	19.4%	No	Yes
1	on demand (1-Ø-Ø)	120	20.25	2.8%	No	No
2	on demand (1-Ø-Ø)	120	40.5	4.4%	No	Yes
5	on demand (1-Ø-Ø)	120	101.24	7.6%	Yes	Yes
10	on demand (1-Ø-Ø)	120	202.47	10.3%	Yes	Yes
0.25	on demand (2-1-1)	192	13.19	0.9%	No	Yes
0.5	on demand (2-1-1)	192	26.37	3.8%	Yes	Yes
0.75	on demand (2-1-1)	192	39.56	5.5%	Yes	Yes
1	on demand (2-1-1)	192	52.75	6.9%	Yes	Yes
2	on demand (2-1-1)	192	105.49	10.4%	Yes	Yes
5	on demand (2-1-1)	192	263.72	20.7%	Yes	Yes
48	Implant	2016	6.51	0.0%	No	No
52	Implant	2016	9.2	0.0%	No	No
54	Implant	2016	10.27	0.1%	No	No
56	Implant	2016	11.83	0.2%	Yes	Yes
62	Implant	2016	15.71	0.2%	Yes	Yes

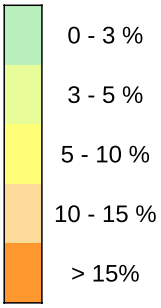

Note: The column "Time above threshold" was used to determine the toxicological risks of the investigated regimen: It depicts the fraction of time that the plasma ISL concentration at steady state is above a no-observed-adverse-effect-level (NOAEL) of 7.02 nM, with a traffic-light related risk grading (green = safe, red = toxic).

while 0.25 mg (non-toxic) achieved $\varphi > 90\%$ after five dosing events and 0.5 mg after three dosing events. However, 0.5 mg may lead to lymphocyte drops, according to our 'time-over-NOAEL' analysis (Table 2).

If taken once weekly at least 5 mg are necessary to achieve > 90% protection. However, this dosing regimen is associated with 5% of time-over-NOAEL. If ISL is taken every second week, 10 mg would be required, with 4% of

21638306, 2024, 10, Downloaded from https://ascpt.onlinelibrary.wiley.com/doi/10.1002/psp4.13212 by Robert Koch-Institut, Wiley Online Library on [28/04/2026]. See the Terms and Conditions (https://onlinelibrary.wiley.com/terms-and-conditions) on Wiley Online Library for rules of use; OA articles are governed by the applicable Creative Commons License

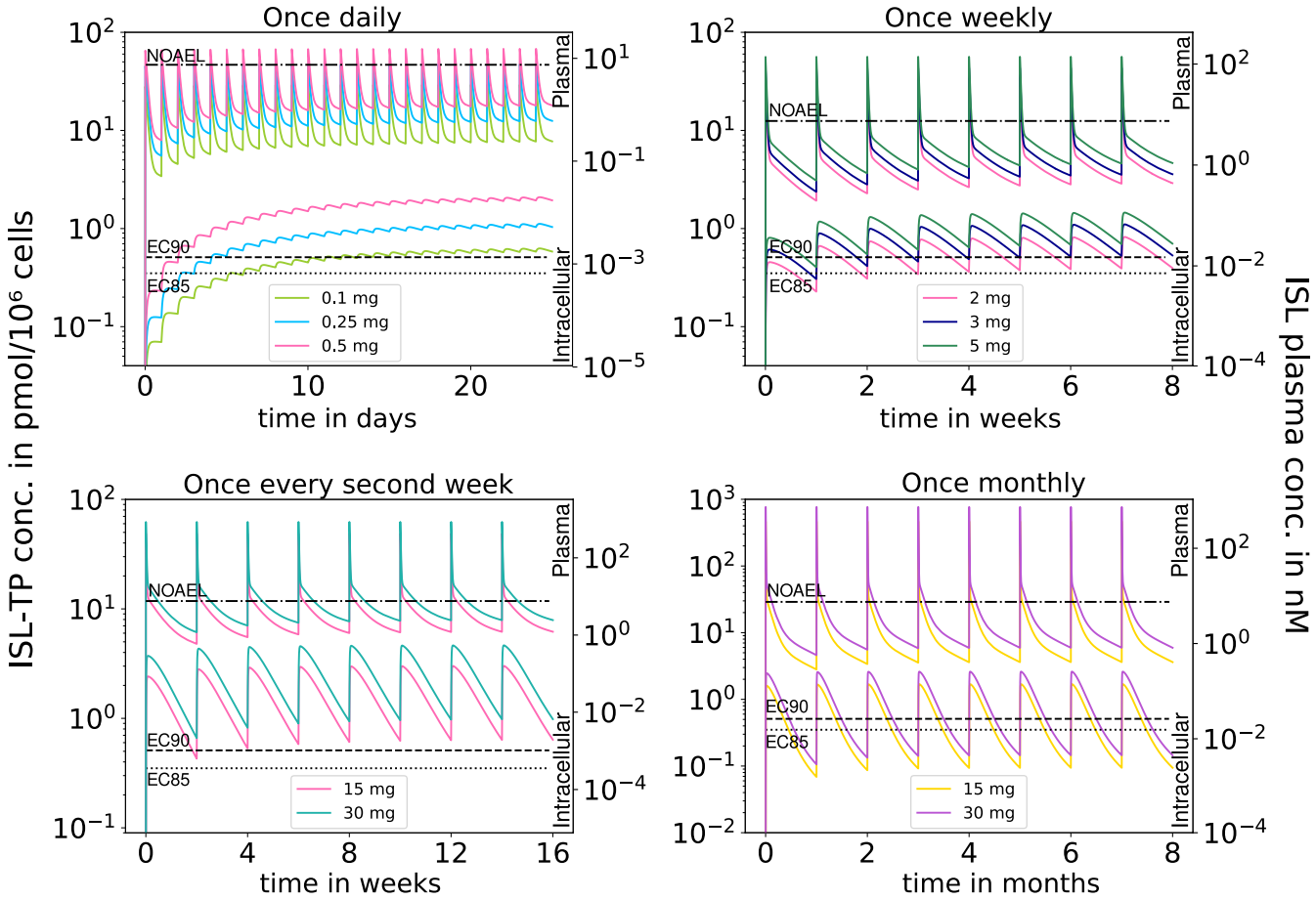

FIGURE 3 Predicted pharmacokinetics for once-daily, −weekly, −biweekly and -monthly oral ISL dosing schedules. Colored lines represent the simulated concentrations in plasma (top half of the figures, right *y*-axes) and intracellular (bottom half, left *y*-axes) of different drug amounts for the respective dosing schedules, which are considered non-toxic (according to our findings in Table 2). The horizontal dashed lines indicate either the NOAEL threshold in plasma or the model-computed 85% and 90% HIV-protective intracellular ISL-TP concentrations (EC_{85} and EC_{90}).

time-over-NOAEL. For monthly dosing, at least 30 mg needs to be taken, but ISL-TP trough levels may fall under the 90% protective threshold. Moreover, the monthly dosing regimen would be associated with substantial time-over-NOAEL (Table 2).

Prophylactic efficacy and toxicity of an on-demand regimen around the time of exposure

Established on-demand PrEP[9,40] dosing patterns with FTC/TDF for MSM consist of a double dose followed by two pills on consecutive days (2 – 1 – 1). In our simulations, we also investigated the efficacy profile of single oral doses (1 – Ø – Ø).

Figure 4a, shows prophylactic efficacy profiles when viral challenge occurred shortly before (PEP), or after (PrEP) the first dose at time point $t = 0$ in the on-demand regimens. The time points at which a regimen falls below an efficacy threshold are shown by black-dashed vertical lines. Notably, an on-demand regimen could circumvent toxic effects, since plasma ISL may only stay above NOAEL for very short times, or does not even reach NOAEL.

According to our simulations, a single ingestion of 2 mg oral ISL would give rise to > 85% prophylactic efficacy almost immediately if taken at the same time as virus exposure or up to 2.5 days prior to the exposure event but never reaches 90%. A single oral 5 mg tablet ISL would reach protective levels of > 90% similarly fast after dosing but would remain protective for about 5 days. Both dosing regimens would give rise to plasma ISL levels that are above NOAEL for 4.4% and 7.6% of the time, see Table 2.

For the 2 – 1 – 1 regimen, only oral doses of 0.5, 1 mg or above would yield >90% efficacy. For 0.5 mg, this level of protection is only achieved if virus exposure occurred at least 3 hours after the first dose. A prophylactic efficacy >90% is maintained for 6 vs. more than 8 days after the last dose with 0.5 and 1 mg, respectively, during 2 – 1 – 1 on-demand dosing. However, both dosages lead to substantial

21638306, 2024, 10, Downloaded from https://ascpt.onlinelibrary.wiley.com/doi/10.1002/psp4.13212 by Robert Koch-Institut, Wiley Online Library on [28/04/2026]. See the Terms and Conditions (https://onlinelibrary.wiley.com/terms-and-conditions) on Wiley Online Library for rules of use; OA articles are governed by the applicable Creative Commons License

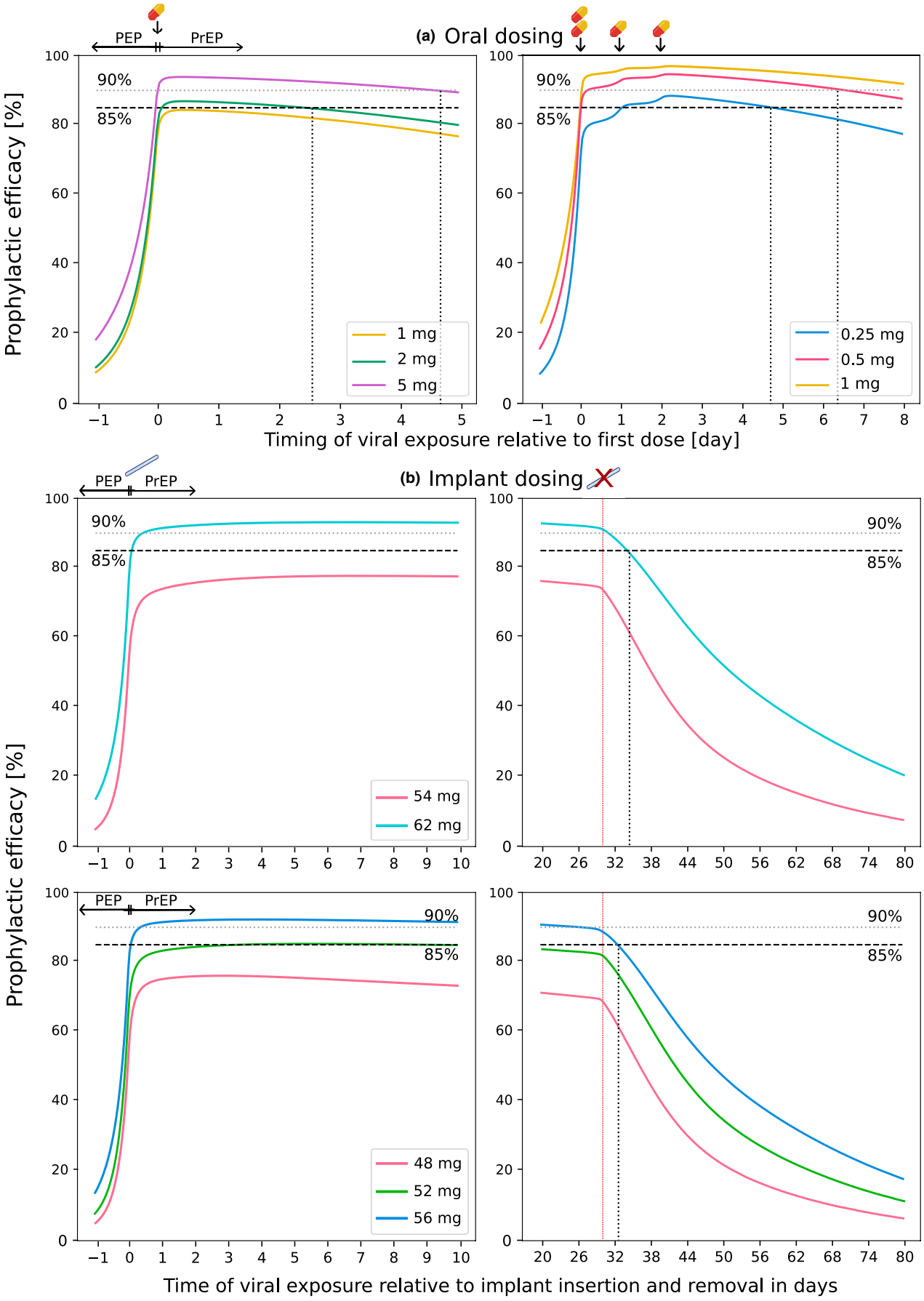

21638306, 2024, 10, Downloaded from https://ascpt.onlinelibrary.wiley.com/doi/10.1002/psp4.13212 by Robert Koch-Institut, Wiley Online Library on [28/04/2026]. See the Terms and Conditions (https://onlinelibrary.wiley.com/terms-and-conditions) on Wiley Online Library for rules of use; OA articles are governed by the applicable Creative Commons License

FIGURE 4 Prophylactic efficacy of oral on-demand dosing and implant administration around the time of virus exposure. (a) Prophylactic efficacy of oral $1-\emptyset-\emptyset$ and $2-1-1$ dosing schemes around the time of virus exposure (indicated on the *x*-axis). (b) Prophylactic efficacy of subcutaneous implants shortly after insertion and removal. The removal of the implants is shown as red vertical lines. The *x*-axis indicates the time of virus exposure, relative to the first dosing event (or implant insertion event). Prophylactic efficacy values of $\varphi = 85\,\%$ and $\varphi = 90\,\%$ are depicted as dashed and dotted horizontal lines, respectively. Vertical black-dotted lines indicate the time when a considered regimen falls below an efficacy threshold.

time (3.8% vs. 6.9%) above NOAEL (Table 2). Furthermore, we observe that all considered dosages are too low to provide sufficient post-exposure prophylactic (PEP) efficacy, while larger dosages could cause adverse effects and were therefore not considered.

Prophylactic efficacy and toxicity of ISL implants

We simulated the prophylactic efficacy of implants loaded with 48, 52, 54, 56, and 62 mg with emphasis on the time shortly after implant insertion ('how quickly is protection achieved?') and after implant removal, Figure 4b. According to our simulations, all considered drug loads lead to plasma ISL exposures smaller than the NOAEL, Table 2. Drug loads greater than 56 mg ISL would give rise to > 90% protection as early as a few hours after implant insertion. After implant removal, the loading dose of 62 mg falls below the 90% efficacy threshold after about 1.5 days and below the 85% threshold after more than 4 days.

DISCUSSION

Adherence to daily oral PrEP is challenging and may limit its uptake. Injectable CAB-LA may overcome daily dosing requirements, but the necessity of frequent injections along with suboptimal drug access may constrain its global impact on HIV prevention. ISL implants represent an entirely novel option for HIV prevention and could contribute to satisfying unmet PrEP-needs.[41,42] While dose-ranging clinical studies on HIV prophylaxis are unrealistic,[10] our modeling of various dosing regimen suggests that ISL implants with 56–62 mg may be safe and effective against HIV transmission.

Notably, our analysis was restricted to publicly available PK data without access to individual-level data, precluding the investigation of covariate relationships for PK and PD using a nonlinear mixed-effects approach. Instead, we utilized an approach based on average pharmacokinetics and explored variability within the dataset using parametric bootstrap techniques (see *Methods*).

The developed PK model represents two dosing routes (oral and subcutaneous implant) and comprises three compartments with an additional intracellular effect compartment (Figure 1a). According to this model, the ISL concentration–time profile in plasma exhibits three phases: In the first phase, the drug concentration enters the plasma and partially diffuses into the peripheral compartments ($C \to P_2 > C \to P_1$). The second phase is characterized by the flux into the first peripheral compartment ($C \to P_1$). The final phase denotes a quasi-steady state where plasma ISL elimination is dominated by the rate-limiting flux from $P_1 \to C$ (Figure S3).

We observed dose-proportional plasma PK (oral doses of 0.5–400 mg, Figure 1c), consistent with [18]. Implant dosing resulted in an initial sharp decline in plasma ISL, transitioning into a very slow decay after about 24 h. The sharp decline was best modeled by an initial drug concentration in the subcutaneous compartment after implant insertion (details see *Methods, PK modeling*), possibly arising from minor injuries at the implant insertion site. Plasma ISL concentrations for the subcutaneous implant were associated with dose, but not necessarily be dose-proportional.

Intracellular ISL-TP did not show proportionality to plasma ISL at higher oral doses (≥30 mg, Table S2). However, we constructed a nonlinear function that modeled the relationship between cellular uptake, intracellular anabolism $\left(k_{C\to E}\right)$, and plasma concentrations for oral dosing (Figure S6) to interpolate between oral dosing regimens. The active moiety ISL-TP had an intracellular half-life of 87.75 h in our model, aligning with literature findings[19] of 78.5–128 h for oral dosages of 0.5–30 mg. The long half-life of ISL-TP allows for sparse dosing, as evaluated in Figure 3. To validate our PK model, we simulated two oral regimens that were not included in parameter estimation. Figure S2 shows overall satisfactory match, particularly for the low-dose regimen, which was the focus of this study.

For implants, intracellular ISL-TP concentration data were not directly correlated with drug loading. The available data showed that the ISL-TP concentration for 52 mg exceeded that of 54 mg (Figure 1b). However, this observation may be linked to an experimental artifact. In our evaluations of prophylactic efficacy, 52 and 54 mg resulted in suboptimal HIV protection (< 90%) and were not considered further.

Following PK model construction and parameterization, we used clinical phase II data to estimate the remaining free parameter (antiviral potency IC_{50} of ISL-TP). Specifically, we used VL data following single oral doses of 0.5–30 mg ISL reported in [19] and estimated $IC_{50} = 429.707$ nM, Figure 2.

21638306, 2024, 10, Downloaded from https://ascpt.onlinelibrary.wiley.com/doi/10.1002/psp4.13212 by Robert Koch-Institut, Wiley Online Library on [28/04/2026]. See the Terms and Conditions (https://onlinelibrary.wiley.com/terms-and-conditions) on Wiley Online Library for rules of use; OA articles are governed by the applicable Creative Commons License

Recently, it was reported that once-daily administration of 0.75 mg ISL leads to a reversible reduction in lymphocyte counts compared with other antiretroviral drugs.[43] While historically, the inhibition of human DNA polymerases (in particular mitochondrial polymerase γ) is associated with NRTI toxicity,[15,44] ISL does not inhibit human DNA polymerase γ.[43] Sequential intracellular phosphorylation by cellular kinases is essential for the biological activation of the drug within HIV target cells. The same enzymes are also used to phosphorylate endogenous nucleosides required for cell metabolism and proliferation. In line with recent discussions on potential mechanisms of NRTI toxicity, the toxic effect of ISL may be due to competition (and inhibition) with endogenous nucleosides for phosphorylation in lymphocytes.[45–47] Notably, a similar mechanism was observed regarding the cardiac toxicity of the NRTI zidovudine (AZT)[48] and denotes the mechanistic basis of synergy between the NRTIs tenofovir and emtricitabine.[16] In both examples, the effect strength (toxicity, synergy) correlates with plasma pro-drug concentrations. Since ISL is a high-affinity substrate for import and phosphorylation in lymphocytes, it may be reasonable to assume that a metabolic predecessor of ISL-TP interferes with cellular (deoxy-)nucleo(s/t)ide pools as a causative mechanism of mild lymphopenia.[49] Consequently, we assumed that plasma ISL is a correlate of $CD4^+$ and lymphocyte reductions.

To identify maximal ISL concentrations that do not cause adverse effects, we replicated dosing scenarios previously examined for lymphocyte count reduction.[37,39] At 0.25 mg oncedaily, we identified a NOAEL threshold of 7.02 nM. Subsequently, we determined the fraction of time, for a given dosing schedule, during which plasma ISL exceeded the NOAEL. This approach indicates a very strict (cautious, conservative) assessment of potential toxicity (an AUC-based alternative is presented in Table 2). Notably, while at most "mild" lymphopenia[37] was observed in some individuals, the strict approach used herein aims at no measurable adverse effects, which is reasonable in the context of PrEP (healthy individuals).

Based on the integrated PK-PD-viral dynamics model, we performed simulations to evaluate prophylactic efficacy after oral or implant dosing. For these simulations, we focused on regimens that would achieve sufficient protection ($\varphi > 85\%$ and $\varphi > 90\%$) and minimize risks of lymphopenia, as outlined above.

Simulation of once-daily oral ISL at sub-NOAEL doses of 0.1 and 0.25 mg predicted 90% prophylactic efficacy, with the 0.25 mg regimen requiring less than daily adherence (4/7 pills achieved $\varphi > 90\%$, see Figure S7). Compared with established oral PrEP with FTC/TDF, the adherence-efficacy profile of 0.25 mg may be slightly inferior[10,50,51] and does not offer a unique niche in the prophylactic portfolio. Less frequent dosing schedules (weekly, biweekly, monthly) achieve > 90% protection but entail a residual risk of lymphopenia. On-demand regimens for PrEP/PEP scenarios suggest no effective protection without potential side effects, according to our estimates.

In this evaluation, ISL-TP in PBMCs served as an efficacy marker for HIV PrEP after sexual HIV challenges.[52,53] While PBMCs contain a significant portion of HIV target cells ($CD4^+$ T cells) that are decisive for establishing viral infection, tissue samples primarily consist of non-HIV target cells (e.g., epithelial cells) with minimal tissue-resident $CD4^+$ T cells. Since NRT(T)Is undergo active transport and intracellular conversion by kinases, which may vary in cell-type-specific expression levels, analyzing tissue samples and cell mixtures dominated by cells irrelevant to viral replication may not accurately predict efficacy for this drug class. Consistent with these considerations, recent findings suggest that PBMCs serve as a better efficacy marker for oral FTC/TDF-based PrEP compared with local tissue concentrations in case of sexual HIV challenge.[10]

Our modeling indicates that subcutaneous ISL implants with at least 56 mg are effective and safe for LA-PrEP, providing prophylactic efficacy while minimizing toxicity risks (0.2% according to our criteria, Table 2). However, the putative toxicity mechanisms and markers for ISL and NRTTIs require further elucidation. The proposed model could be adapted for novel NRTTIs, including Merck's new developmental drug NCT05494736 (MK-8527), to support clinical investigation and identify prophylactic niches.[54]

AUTHOR CONTRIBUTIONS

H.K. and M.v.K. wrote the manuscript with help from C.W.H. and J.H. H.K. and M.v.K. designed the research. H.K. and L.Z. performed the research and H.K., C.W.H., J.H., and M.v.K analyzed the data.

ACKNOWLEDGMENTS

H.K., L.Z. and M.v.K. acknowledge funding from the German Ministry for Science and Education (BMBF; grants 01KI2016). The funders had no role in designing the research or the decision to publish. Open Access funding enabled and organized by Projekt DEAL.

CONFLICT OF INTEREST STATEMENT

J.H. has been a consultant for Merck; prior studies have received donated FTC-TDF from Gilead. C.W.H. has received funding for clinical research and been a (past) consultant for Merck, Gilead and ViiV/GSK, holds US patents related to HIV prevention technology (US20200138700A1) and founded Prionde Biopharma, LLC, a microbicide company; all relationships are managed by Johns Hopkins University. All other authors declared no competing interests for this work.

21638306, 2024, 10, Downloaded from https://ascpt.onlinelibrary.wiley.com/doi/10.1002/psp4.13212 by Robert Koch-Institut, Wiley Online Library on [28/04/2026]. See the Terms and Conditions (https://onlinelibrary.wiley.com/terms-and-conditions) on Wiley Online Library for rules of use; OA articles are governed by the applicable Creative Commons License

ORCID

Hee-yeong Kim https://orcid.org/0009-0005-9060-8953
Lanxin Zhang https://orcid.org/0000-0002-3740-4450
Craig W. Hendrix https://orcid.org/0000-0002-5696-8665
Jessica E. Haberer https://orcid.org/0000-0001-5845-3190
Max von Kleist https://orcid.org/0000-0001-6587-6394

REFERENCES

1. Barré-Sinoussi F, Chermann JC, Rey F, et al. Isolation of a T-lymphotropic retrovirus from a patient at risk for acquired immune deficiency syndrome (AIDS). *Science*. 1983;220(4599):868-871.
2. Gallo RC. *Virus Hunting: AIDS, Cancer, and the Human Retrovirus: A Story of Scientific Discovery*. BasicBooks; 1991.
3. Fact sheet – Latest global and regional statistics on the status of the AIDS epidemic. https://www.unaids.org/sites/default/files/media_asset/UNAIDS_FactSheet_en.pdf. Accessed January 06, 2023.
4. UNAIDS Global AIDS. Update 2022. https://www.unaids.org/sites/default/files/media_asset/2022-global-aids-update-summary_en.pdf. Accessed January 04, 2023.
5. Grant RM, Lama JR, Anderson PL, et al. Preexposure chemoprophylaxis for HIV prevention in men who have sex with men. *New Engl J Med*. 2010;363(27):2587-2599.
6. Baeten JM, Palanee-Phillips T, Brown ER, et al. Use of a vaginal ring containing dapivirine for hiv-1 prevention in women. *New Engl J Med*. 2016;375(22):2121-2132.
7. Schmidt D, Duport Y, Kollan C, Marcus U, Iannuzzi S, von Kleist M. Dynamics of HIV prep use and coverage during and after Covid-19 in Germany. 10.2139/ssrn.4611490 2023.
8. Molina J-M, Capitant C, Spire B, et al. On-demand preexposure prophylaxis in men at high risk for HIV-1 infection. *New Engl J Med*. 2015;373(23):2237-2246.
9. Molina J-M, Ghosn J, Assoumou L, et al. Daily and on-demand HIV pre-exposure prophylaxis with emtricitabine and tenofovir disoproxil (ANRS PREVENIR): a prospective observational cohort study. *Lancet HIV*. 2022;9(8):e554-e562.
10. Zhang L, Iannuzzi S, Chaturvedula A, et al. Model-based predictions of protective hiv pre-exposure prophylaxis adherence levels in cisgender women. *Nat Med*. 2023;29:1-10.
11. World Health Organization. *Differentiated and Simplified Pre-Exposure Prophylaxis for HIV Prevention: Update to WHO Implementation Guidance: Technical Brief*. WHO; 2022.
12. Delany-Moretlwe S, Hughes JP, Bock P, et al. Cabotegravir for the prevention of HIV-1 in women: results from HPTN 084, a phase 3, randomised clinical trial. *Lancet*. 2022;399(10337):1779-1789.
13. Diamond TL, Ngo W, Min X, et al. Islatravir has a high barrier to resistance and exhibits a differentiated resistance profile from approved nucleoside reverse transcriptase inhibitors (NRTIs). *Antimicrob Agents Chemother*. 2022;66(6):e00133-22.
14. Pons-Faudoa FP, Di Trani N, Capuani S, et al. Long-acting refillable nanofluidic implant confers protection against shiv infection in nonhuman primates. *Sci Transl Med*. 2023;15(702):eadg2887.
15. von Kleist M, Metzner P, Marquet R, Schütte C. HIV-1 polymerase inhibition by nucleoside analogs: cellular-and kinetic parameters of efficacy, susceptibility and resistance selection. *PLoS Comput Biol*. 2012;8(1):e1002359.
16. Iannuzzi S, von Kleist M. Mathematical modelling of the molecular mechanisms of interaction of tenofovir with emtricitabine against HIV. *Viruses*. 2021;13(7):1354.
17. Michailidis E, Huber AD, Ryan EM, et al. 4′-Ethynyl-2-fluoro-2′-deoxyadenosine (EFdA) inhibits HIV-1 reverse transcriptase with multiple mechanisms. *J Biol Chem*. 2014;289(35):24533-24548.
18. Matthews RP, Ankrom W, Friedman E, et al. Safety, tolerability, and pharmacokinetics of single-and multiple-dose administration of islatravir (mk-8591) in adults without hiv. *Clin Transl Sci*. 2021;14(5):1935-1944.
19. Schürmann D, Rudd DJ, Zhang S, et al. Safety pharmacokinetics, and antiretroviral activity of islatravir (ISL MK-8591), a novel nucleoside reverse transcriptase translocation inhibitor, following single-dose administration to treatment-naive adults infected with HIV-1: an open-label, phase 1b, consecutive-panel trial. *Lancet HIV*. 2020;7(3):e164-e172.
20. Matthews RP, Patel M, Barrett SE, et al. Safety and pharmacokinetics of islatravir subdermal implant for hiv-1 pre-exposure prophylaxis: a randomized, placebo-controlled phase 1 trial. *Nat Med*. 2021;27(10):1712-1717.
21. Kirby KA, Michailidis E, Fetterly TL, et al. Effects of substitutions at the 4′ and 2 positions on the bioactivity of 4′-ethynyl-2-fluoro-2′-deoxyadenosine. *Antimicrob Agents Chemother*. 2013;57(12):6254-6264.
22. Salie ZL, Kirby KA, Michailidis E, et al. Structural basis of HIV inhibition by translocation-defective RT inhibitor 4′-ethynyl-2-fluoro-2′-deoxyadenosine (EFdA). *Proc Natl Acad Sci*. 2016;113(33):9274-9279.
23. Takamatsu Y, Das D, Kohgo S, et al. The high genetic barrier of EFdA/MK-8591 stems from strong interactions with the active site of drug-resistant HIV-1 reverse transcriptase. *Cell Chemical Biology*. 2018;25(10):1268-1278.
24. Merck Announces Clinical Holds on Studies Evaluating Islatravir for the Treatment and Prevention of HIV-1 Infection. https://www.merck.com. Accessed March 10, 2023.
25. Merck restarts islatravir HIV treatment studies, but abandons monthly PrEP. https://www.merck.com. Accessed March 10, 2023.
26. Trials of long-acting islatravir for HIV treatment and prevention placed on hold. https://www.aidsmap.com/news/dec-2021/trials-long-acting-islatravir-hiv-treatment-and-prevention-placed-hold. Accessed March 10, 2023.
27. Merck Provides Update on Phase 2 Clinical Trial of Once-Weekly Investigational Combination of MK-8507 and Islatravir for the Treatment of People Living with HIV-1. https://www.merck.com. Accessed March 10, 2023.
28. Barrett SE, Teller RS, Forster SP, et al. Extended-duration MK-8591-eluting implant as a candidate for HIV treatment and prevention. *Antimicrob Agents Chemother*. 2018;62(10):e01058-18.
29. Duwal S, Schütte C, von Kleist M. Pharmacokinetics and pharmacodynamics of the reverse transcriptase inhibitor tenofovir and prophylactic efficacy against HIV-1 infection. *PLoS One*. 2012;7(7):e40382.
30. Duwal S, von Kleist M. Top-down and bottom-up modeling in system pharmacology to understand clinical efficacy: an example with NRTIs of HIV-1. *Eur J Pharm Sci*. 2016;94:72-83.

21638306, 2024, 10, Downloaded from https://ascpt.onlinelibrary.wiley.com/doi/10.1002/psp4.13212 by Robert Koch-Institut, Wiley Online Library on [28/04/2026]. See the Terms and Conditions (https://onlinelibrary.wiley.com/terms-and-conditions) on Wiley Online Library for rules of use; OA articles are governed by the applicable Creative Commons License

31. Matthews RP, Zang X, Barrett SE, et al. A randomized double-blind, placebo-controlled, phase 1 trial of radiopaque Islatravir-eluting subdermal implants for pre-exposure prophylaxis against HIV-1 infection. *J Acquir Immune Defic Syndr*. 2022;92(4):310-316.
32. Duwal S, Sunkara V, von Kleist M. Multiscale systems-pharmacology pipeline to assess the prophylactic efficacy of NRTIs against HIV-1. *CPT Pharmacometrics Syst Pharmacol*. 2016;5(7):377-387.
33. Zhang L, Wang J, von Kleist M. Numerical approaches for the rapid analysis of prophylactic efficacy against HIV with arbitrary drug-dosing schemes. *PLoS Comput Biol*. 2021;17(12): e1009295.
34. Keele BF, Giorgi EE, Salazar-Gonzalez JF, et al. Identification and characterization of transmitted and early founder virus envelopes in primary hiv-1 infection. *Proc Natl Acad Sci*. 2008;105(21):7552-7557.
35. Matthews RP, Rudd DJ, Zhang S, et al. Safety and pharmacokinetics of once-daily multiple-dose administration of islatravir in adults without hiv. *J Acquir Immune Defic Syndr*. 2021;88(3):314-321.
36. Grobler JA, Lai M-T, Barrett SE, et al. Islatravir PK threshold & dose selection for monthly oral HIV-1 PrEP. *Conference on Retroviruses and Opportunistic Infections (CROI)*, March 2021, Virtual Meeting.
37. Squires KE, Correll TA, Robertson MN, et al. Effect of Islatravir on total lymphocyte and lymphocyte subset count. *Conference on Retroviruses and Opportunistic Infections (CROI)*. February 2023, Seattle, Washington. 2023.
38. Duwal S, Dickinson L, Khoo A, von Kleist M. Mechanistic framework predicts drug-class specific utility of antiretrovirals for HIV prophylaxis. *PLoS Comput Biol*. 2019;15(1):e1006740.
39. Grobler JA, Lai M-T, Barrett SE, et al. Modeling and simulation to optimize Islatravir once daily (QD) Doses in HIV Treatment Naive and Virologically Suppressed Populations. *HIV Glasgow 2022*. Virtual Meeting. 2022.
40. Antoni G, Tremblay C, Delaugerre C, et al. On-demand pre-exposure prophylaxis with tenofovir disoproxil fumarate plus emtricitabine among men who have sex with men with less frequent sexual intercourse: a post-hoc analysis of the anrs ipergay trial. *Lancet HIV*. 2020;7(2):e113-e120.
41. Greene GJ, Swann G, Fought AJ, et al. Preferences for long-acting pre-exposure prophylaxis (prep), daily oral prep, or condoms for hiv prevention among us men who have sex with men. *AIDS Behav*. 2017;21:1336-1349.
42. Haberer JE, Mujugira A, Mayer KH. The future of hiv pre-exposure prophylaxis adherence: reducing barriers and increasing opportunities. *Lancet HIV*. 2023;10:e404-e411.
43. Lebron JA, Sobol Z, Barnum J, et al. Ernest Asante-Appiah and Sandrine Ferry-Martin. Investigational studies to understand the decreases in lymphocytes seen clinically with Islatravir (ISL) and enabling 1the initiation of new clinical trials. *19th European AIDS Conference*, October 2023, Warsaw, Poland.
44. Kakuda TN. Pharmacology of nucleoside and nucleotide reverse transcriptase inhibitor-induced mitochondrial toxicity. *Clin Ther*. 2000;22(6):685-708.
45. Holec AD, Mandal S, Prathipati PK, Destache CJ. Nucleotide reverse transcriptase inhibitors: a thorough review, present status and future perspective as hiv therapeutics. *Curr HIV Res*. 2017;15(6):411-421.
46. Anderson PL, Kakuda TN, Lichtenstein KA. The cellular pharmacology of nucleoside-and nucleotide-analogue reverse-transcriptase inhibitors and its relationship to clinical toxicities. *Clin Infect Dis*. 2004;38(5):743-753.
47. Ray AS. Intracellular interactions between nucleos (t) ide inhibitors of HIV reverse transcriptase. *AIDS Rev*. 2005;7(2):113-125.
48. Susan-Resiga D, Bentley AT, Lynx MD, LaClair DD, McKee EE. Zidovudine inhibits thymidine phosphorylation in the isolated perfused rat heart. *Antimicrob Agents Chemother*. 2007;51(4):1142-1149.
49. Shepard C, Joella X, Holler J, et al. Effect of induced dNTP pool imbalance on HIV-1 reverse transcription in macrophages. *Retrovirology*. 2019;16(1):1-11.
50. Anderson PL, Marzinke MA, Glidden DV. Updating the adherence–response for oral emtricitabine/tenofovir disoproxil fumarate for human immunodeficiency virus pre-exposure prophylaxis among cisgender women. *Clin Infect Dis*. 2023;76(10):1850-1853.
51. Moore M, Stansfield S, Donnell DJ, et al. Efficacy estimates of oral pre-exposure prophylaxis for hiv prevention in cisgender women with partial adherence. *Nat Med*. 2023;29:1-5.
52. Matthews RP, Rudd DJ, Levine V, et al. Multiple daily doses of MK-8591 as low as 0.25 mg are expected to suppress HIV. *Conference on Retroviruses and Opportunistic Infections (CROI)*, March, 2018, Boston, Massachusetts.
53. Craig W, Hendrix SH, Bekker L-G, et al. Islatravir distribution in mucosal tissues, PBMC & plasma after monthly oral dosing. *Conference on Retroviruses and Opportunistic Infections (CROI)*, Abstract 83, February 2022, Virtual Conference.
54. Haberer JE, Bangsberg DR, Baeten JM, et al. Defining success with hiv pre-exposure prophylaxis: a prevention-effective adherence paradigm. *AIDS (London, England)*. 2015;29(11):1277.
55. Rudd DJ, Zhang S, Fillgrove KL, et al. Lack of a clinically meaningful drug interaction between the HIV-1 antiretroviral agents Islatravir dolutegravir, and tenofovir disoproxil fumarate. *Clin Pharmacol Drug Develop*. 2021;10(12):1432-1441.

SUPPORTING INFORMATION

Additional supporting information can be found online in the Supporting Information section at the end of this article.

How to cite this article: Kim H-y, Zhang L, Hendrix CW, Haberer JE, von Kleist M. Modeling of HIV-1 prophylactic efficacy and toxicity with islatravir shows non-superiority for oral dosing, but promise as a subcutaneous implant. *CPT Pharmacometrics Syst Pharmacol*. 2024;13:1693-1706. doi:10.1002/psp4.13212

21638306, 2024, 10, Downloaded from https://ascpt.onlinelibrary.wiley.com/doi/10.1002/psp4.13212 by Robert Koch-Institut, Wiley Online Library on [28/04/2026]. See the Terms and Conditions (https://onlinelibrary.wiley.com/terms-and-conditions) on Wiley Online Library for rules of use; OA articles are governed by the applicable Creative Commons License